TRIUMF Beam Physics Note
TRI-BN-22-21
May 27, 2022

Design of Innovative Superconducting Cyclotron TR100+ for Commercial Isotopes Production

Y.-N. Rao and L.G. Zhang

TRIUMF

Abstract: This note summarizes a baseline design of TR100+, an innovative superconducting cyclotron for 300 MeV H_2^+ beam, by strippping extraction to deliver protons up to 150 MeV.

4004 Wesbrook Mall, Vancouver, B.C. Canada V6T 2A3 · Tel: 604 222-1047 · Fax: 604 222-1074 · www.triumf.ca

1 Objectives

Our objective is to investigate the feasibility of a new type of compact superconducting cyclotron that could use the technique of stripping hydrogen molecular ions H_2^+ or H_3^+ to extract protons. By stripping, it's meant that the H_2^+ or H_3^+ ions simply pass through a thin carbon foil, which strips off the electron(s), producing 2 or 3 protons. To make a cyclotron compact, higher fields are necessary, but this eliminates the option of using H^- as accelerated particle. Instead, the new technique uses H_2^+ or H_3^+ ions as these can possibly tolerate much higher magnetic field. This is an innovative method [1] [2], allowing the use of superconducting (SC) coils and the development of a new class of intermediate to high energy cyclotrons to deliver high intensity proton beam. Our study concentrates on the beam physics aspects especially on the feasibility of extraction in terms of beam losses; these must be minimized to avoid activation of the machine and to allow for hands-on maintenance, because the major limitation on the operation of high current cyclotrons is imposed by the extraction losses.

We focus on the proton energy of $70 - 150\,\mathrm{MeV}$ and proton current of $\sim 1\,\mathrm{mA}$, because cyclotron in this energy range is not developed world-wide; and more importantly, in the energy range up to 150 MeV numerous highly interested and increasingly demanded radionuclides can be produced for RIB physics researches, and as parent nuclei for generator use or directly as an active pharmaceutical ingredient. For example, the proton bombardment of thorium targets [5] yields a treasure trove of products such as Actinium-225 (Ac-225), Bismuth-213 (Bi-223), Radium-225 (Ra-225) and Astatine-211 (As-211), etc; the production cross-section reaches a plateau as the proton incident energy gets to about 150 MeV. With additional development, access to other valuable isotopes such as Ra-224, Pb-212 and Bi-212 are possible. The isotopes Ac-225 and Bi-213 are anticipated to drive radio-pharmaceutical developments for the researches of cancers (Melanoma, Prostate and Pancreatic) conducted at the British Columbia Cancer Agency (BCCA) in Canada, and to expand in the leading radionuclide imaging program. Another example, the isotope Strontium-82 (Sr-82) is used exclusively to manufacture the generators of Rubidium-82 (Rb-82) which is the most convenient Positron Emission Tomography (PET) agent in myocardial perfusion imaging. Over the last 15 years, the demand for Sr-82 from pharmaceutical industry has been growing, and such a demand is anticipated to continue to grow for the next 20 years. To date, all the Sr-82 are produced at large facilities which are primarily used for scientific researches. Cyclotron is one of these, for example the TRIUMF 500 MeV H^- cyclotron, but none of them is dedicated for the Sr-82 production.

Utilizing dedicated cyclotrons to produce medical isotopes is an arising technology in hospitals across Canada. An excellent example is that in January 2015, the CycloMed99 team [6], led by TRIUMF, demonstrated a breakthrough in producing the world's most highly used medical isotope, technetium-99m (Tc-99m), on existing medical cyclotrons [7, 8] so that eliminates the crisis [9] of an isotope shortage. This solution enables Canada to use cyclotrons to implement the direct production of Tc-99m without nuclear reactors and without uranium, while providing a safe and secure supply chain of this lifesaving isotope for local hospitals and clinics. No doubt that the cyclotrons as a local infrastructure play an essential role.

In terms of the proton current specification, our project is at the technological edge of the cyclotrons being constructed today. We aim for a cyclotron that combines two great virtues, i.e. compactness and potentials of simultaneously providing multiple proton beams for multiple external production targets of variable currents by means of stripping extraction.

2 Overview

There are two major types of commercial medical cyclotrons [10] in the global market: one is for medical isotopes production, the other is for proton therapy. The former ones are typically high-current low-energy (i.e. 1 mA, 7−30 MeV) H^- machines, while the latter are low-current high-energy (i.e. 1 µA, 200−400 MeV) proton machines. For either type, there are several well-established vendors [10] in the market, namely IBA, ACSI, GE, Varian, Siemens, Sumitomo and Still River, as well as the emerging players such as BEST (Canada) and CIAE (China). From this overview it becomes apparent that the 7−30 MeV and 200−400 MeV energy range cyclotrons are well covered in the market by multiple strong players. But, contrastingly, the 70−150 MeV energy range is not well represented; there being only few outliers at 70 and 100 MeV: the BEST Cyclotron 70P (in Legnaro, Italy) [11], the IBA C70 (in Nantes, France) [12] and the CYCIAE-100 in Beijing [13]. All these are accelerating H^- to extract protons by stripping, in which a dominant factor limiting the beam intensity is the beam loss due to the electromagnetic stripping (Lorentz stripping) of the second electron during acceleration [14]. To reduce activation of the accelerator system, caused by the resulting beam spills, the losses have to be kept low. This requires the magnetic field to be lower, the higher the machine energy, which in turn leads to the larger magnet size. Since the cost of the cyclotron rises with magnet size, the commercial H^- cyclotron balances acceptable losses versus size, ending up at a compromised energy of ∼70 MeV [15].

For example, the BEST 70 MeV cyclotron has B_0 of 0.922 T in the machine centre, a maximum field of 0.991 T in average and a maximum field of 1.60 T in the hill. The yoke outer diameter is 4.5 m and the total weight is 190 tons. This machine is even larger than the PSI 250 MeV superconducting cyclotron [16] of only 3.2 m in diameter, and is 2 times heavier than the latter. Thus, the BEST 70P is not really a compact machine.

Another example, the CYCIAE-100 [13], a 100 MeV machine, has B_0 of 0.71 T, a maximum field of 0.7 T in average and a maximum field of 1.35 T in the hill. The magnet pole diameter is 4 m while the yoke outer diameter is 6.16 m; the total weight exceeds 400 tons. This is not a compact machine either.

The commercial superconducting cyclotrons are becoming ever more compact due to the introduction of successive generations of conductor technology for the magnet windings. The application of superconducting design has two evident advantages [16]. Firstly, the superconducting coils allow the machine to have extremely good reproducibility and linearity in the magnetic field with respect to the coil current changes, because the field-shaping iron and yoke get fully saturated in a strong field (> 2 T) of the coils; there is barely hysteresis effect. The magnetic field is dominated by the coil current. Secondly, the power consumption is at

least 10 times less and the machine's weight is 2 times lighter than any normal-conducting cyclotron [17, 18] of identical energy. However, a small size is not necessarily a virtue. There should be a cost optimum in a design for a medical isotope production machine that adopts more mature and (comparatively) lower field conductor technology.

As for the cyclotrons of directly using protons without stripping, extraction is one of the critical issues, since it's generally performed by electrostatic deflector. To be an efficient process, this extraction method requires well separated orbital turns, which is achieved with a large radius of the machine and a high accelerating voltage [19], making the cyclotron very expensive. The proton machines for therapy (up to $\sim$1 µA extraction) can hardly reach an extraction efficiency of above 80% [16, 18, 20], no matter it's normal-conducting or superconducting. If they were for high current, they would not be able to run safely, because too much beam would get lost at extraction, exacerbating the neutron production and machine activation problem.

To overcome these limitations and reliably deliver high current ($\geq$ 500 µA) proton beam on target, we intend to accelerate H_2^+ (or H_3^+) as they have ground state binding energy of 2.75 eV (or 4.37 eV for H_3^+) [21, 22], much larger than that of H^- (0.75 eV). This implies that a much higher magnetic field could be used in a compact cyclotron with significantly reduced magnet size and consequently lower costs. Moreover, the machine's phase acceptance, similar to the H^- cyclotron, is not limited by requiring all particles to have the same turn history for the extraction. This allows to attain high current.

One of the pros of H_2^+ acceleration is that it reduces space-charge effects. This is easily understood as for every two protons injected at the machine centre, there is only +1 electric charge. Thus, we have 1 mA of H_2^+ while we provide 2 mA of protons to the target. Another pro of the choice of H_2^+ is that the stripping of H_2^+ produces electrons that are bent towards the outer radius of the cyclotron, so an electron catcher can be installed to remove the electrons emerging from the stripper and reduce the stripper damage due to thermal load.

Nevertheless, one of the challenges of using H_2^+ is that, instead of bending towards outside, the protons emerging from the stripper bend inwards too [25], with smaller bend radius of curvature than the circulating H_2^+. Depending on the placement of the stripper in the hill/valley configuration, one could bring the proton beam out in a number of different ways. Selection of the extraction path relies on simulations to calculate optimum beam size and minimum beam loss.

The method of extraction for heavy ions from azimuthally-varying field cyclotrons through the stripping foils was initially suggested by Oganessian et al [26], and was used as a basic method in the FLNR (Dubna) cyclotrons [27]. The stripping extraction of H_2^+ was proposed by Calabretta 20 years ago [1, 2]. Since then, there were studies devoted to the SCENT project [28], and then to the ISODAR and DAEδALUS projects [29, 30]. The former is for 250 MeV proton therapy; the latter is for energy up to 800 MeV/n for neutrino physics research. None of these machines has been built yet, but it's conceived that the H_2^+ cyclotron will come into the market within the next few years because of its advantages.

3 Basic Design Consideration

Our basic consideration for the design of TR100+ are as follows.

- Employ superconducting design for a smaller size, lighter weight, and less power consumption machine. So, a strong field of $\geq$2.0 T is built up to fully saturate the field-shaping iron, thus allow to carry extraordinary good reproducibility and linearity in the field with respect to any coil current changes.
- Keep the Lorentz stripping induced beam loss below 1%. The binding of H_2^+ ion can be dissociated, depending on the magnetic field strength and the particle energy. This issue is complicated by the existence of 19 vibrational excited states of the ions [31], populated at the percent level. In terms of Hiskes' theory [21], we estimate that for an energy of 150 MeV/n and a field strength of 2.5 Tesla (maximum), the H_2^+ ions in the vibrational states of $\nu \geq 16$ would dissociate, leading to about 0.5% beam loss into the vacuum. This is not necessarily unacceptable, however.
- Replicate the geometry and size of the TR30 centre region [32], because the TR30 centre region is a highly optimized design for the parameters of $R_\infty = 2.6$ m and injection energy of 25 keV (H^-) as well as dee voltage of 50 kV. This is to say, we keep $\overline{R} = \beta R_\infty$ identical between these two machines over the first 2−3 turns.

To this end, we can scale up the parameters of TR30 for the TR100+, in terms of the ratio of B_0 (in the centre) of these two machines and the ratio of the accelerated particle's rest mass. See Table 3. Note that the choice of B_0 =2.0 or 3.0 T for the TR100+ is kind of arbitrary. In the end it will be a trade-off among all the relevant parameters, taking into account the Lorentz stripping loss and the SC coil's current density limitation, etc. For easy view and comparison, we list the major parameters of several interested machines in Table 3 including TR30, where the PSI 250 MeV SC [33] and TR30 [34] have been operational for years, while the SCENT-300 SC [35] and the IBA C400 SC [36] haven't been built yet. The point to make is that these SC machines are just for lower intensity beam, while the TR30 is normal-conducting machine with high intensity capability demonstrated. We intend to combine the virtues of these two types for the TR100+ design.

In comparison with the proton cyclotron, the H_2^+ machine has to be 2 times larger in the magnet size in order to achieve the same extraction energy protons, given that the two machines have an identical maximum field strength. This is easily understood from the widely used (non-relativistic) formula for the final kinetic energies of the ions produced by the cyclotron, represented as

$$\frac{E_k}{A} = \frac{(e\,\overline{B}\,\overline{R}_{max})^2}{2\,m_a}\left(\frac{q}{A}\right)^2 \equiv K\left(\frac{q}{A}\right)^2 , \tag{1}$$

where E_k is the kinetic energy of the ion with charge number q and mass number A, $\overline{B}$ is the average field on the orbit of maximum average radius $\overline{R}_{max}$, $m_a = 1.6726 \times 10^{-27}$ kg

Table 1: TR100+ parameters scaled up with those of TR30

Parameters	TR30	TR100+ option 1	Ratio TR100+/TR30	TR100+ option 2	Ratio TR100+/TR30
Particle accelerated	H^-	H_2^+		H_3^+	
Charge state q	1	1	1	1	1
Rest mass m (MeV/c^2)	939.277	1876.635	$2 \equiv$ a	2815.209	3
B_0 (at centre) (T)	1.2	2.0	$1.667 \equiv$ b	3.0	2.5
$R_\infty = m\,c/(q\,B_0)$ (m)	2.611	3.133	$1.2 =$ a/b	3.133	1.2
Injection β	0.73%	0.608%	$0.833 =$ b/a	0.608%	0.833
Injection radius					
$\overline{R} = \beta R_\infty$ (cm)	**1.906**	**1.906**	**1**	**1.906**	**1**
Injection kin. energy					
$W = mc^2\beta^2/2$ (keV)	25	34.7	$1.389 = b^2/a$	52.1	2.083
Dee voltage (kV)	50	69.4	$1.389 = b^2/a$	104.2	2.083
RF frequency (MHz)	73	61	$0.833 =$ b/a	61	0.833
Spiral inflector					
Electric radius (Height)					
$A = 2W/(q\,E)$ (cm)	2.5	3.47	$1.389 = b^2/a$	5.21	2.083
Magnetic radius					
$\overline{R} = mc\beta/(qB_0)$ (cm)	1.906	1.906	1	1.906	1
Electrode spacing (mm)	8.0	8.0	1	8.0	1
Electrode potential (kV)	$\pm$8.0	$\pm$8.0	1	$\pm$8.0	1
Electric field (kV/cm)	20.0	20.0	1	20.0	1

$=938.272\,\mathrm{MeV}/c^2$ is the proton mass; for ions $m_a = 1.6605\times10^{-27}$ kg$=931.494\,\mathrm{MeV}/c^2$ is the atomic mass unit. **The parameter $K = 48(\overline{B}\,\overline{R})^2$ in MeV, representing the machine's maximum bending power**, in which $\overline{B}$ and $\overline{R}$ are in Tesla and meter respectively.

Next, we compare the sizes of the H_2^+ and H_3^+ two machines, provided that they have the same energy protons extracted.

- For H_2^+, $\dfrac{q}{A} = \dfrac{1}{2}$, if $B_0 = 2\,\mathrm{Tesla}$, then $\overline{B}_{max} = B_0\,\gamma = 2\,\gamma$;
- For H_3^+, $\dfrac{q}{A} = \dfrac{1}{3}$, if $B_0 = 3\,\mathrm{Tesla}$, then $\overline{B}_{max} = B_0\,\gamma = 3\,\gamma$.

So, from Eq.(1) we get

$$\left(2\,\gamma\overline{R}_{H_2^+}\right)\,\frac{1}{2} = \left(3\,\gamma\overline{R}_{H_3^+}\right)\,\frac{1}{3}\,,$$

which is

$$\overline{R}_{H_2^+} = \overline{R}_{H_3^+}\,,$$

implying an identical extraction radius.

Table 2: Major parameters of interested superconducting isochronous cyclotrons and TR30

Parameters	PSI 250 MeV SC [33]	SCENT-300 SC [35]	IBA C400 SC [36]	TR30 [34]
Particle accelerated	proton	H_2^+, $^{12}C^{6+}$	H_2^+, $^{12}C^{6+}$ ...	H^-
Injection energy (keV/n)	∼0.010	25	12.5	25
I.S. Extraction Voltage (kV)		50	25	25
Injection scheme	Internal PIG	axial with inflector	axial with spiral inflector	axial with spiral inflector
Extraction energy (MeV/n)	250	p @ 260, $^{12}C^{6+}$@300	p@265, $^{12}C^{6+}$@400	30
Extracted current (μA)	≤ 0.8	< 1.0	< 1.0	≥ 1000
Extraction	p by ESD	p by stripping, C by 2 ESDs + 4 passive MCs	p by stripping, C by 1 ESD	p by stripping
Number of sectors	4	4	4	4
Pole diameter (m)	1.63	2.65	3.74	1.52
Iron yoke outer diameter (m)	3.2	5.0	6.6	2.62
Hill gap (cm)	4.0	5.0	elliptical 12 cm at centre decreasing to 1.2 cm at extraction	4.0
B_0 (at centre) (T)	2.38	3.15	2.43	1.20
Maximum average B (T)	3.02	4.20	3.5	1.22
Superconductor Coils	2	2	2	
Current density (A/mm^2)		47		
Number of dees	4	4	2	2
RF harmonic number	2	4	4	4
RF frequency (MHz)	72.8	98	75	73
Dee voltage (kV)	80−130	70−120	80−160	50
Dee tips vert. full aper.(cm)			1.2 cm @1st turn, 2.0 cm @≥2nd turns	1.0 cm @1st dee 2.0 cm @2nd dee and after
Dee gap C.L. angular width (°)			45	45
Spiral inflector				
Height (electric radius) (cm)		4.28	2.5	2.5
Electrode spacing (mm)		6.0	6.0	8.0
Electrode potential (kV)		±7.0	±6.0	±8.0
Electric field (kV/cm)		23.3	20.0	20.0
Electrode width (mm)		12.0	12.0	
Tilt k'			0.1	−0.84

The scale of TR100+ is set by the proton energy (up to 150 MeV), the superconducting technology, the high current (up to 5 mA) H_2^+ external ion source, the stripping of H_2^+ to extract protons (up to 1.0 mA), and the multiple external production targets, etc. A preliminary design was carried out, coming up with a 4-sector compact machine of 3.5 m diameter, 2.0 m height, and 4 deep valleys. The two opposite valleys accommodate rf cavities and the other two house diagnostic elements. Two RF cavities operating in 4th harmonic at a fixed frequency of ∼61 MHz, accelerate the H_2^+ with a maximum dee voltage of 70 kV. Table 3 summarizes the main parameters of a baseline design that we currently consider.

Table 3: TR100+ baseline design primary parameters.

Parameters	Values
Particle accelerated	H_2^+
Extraction energy (MeV/n)	$135 - 150$
Number of sectors	4
Pole radius (cm)	165
Hill gap (cm)	4.5
Mean magnetic field (T)	2.0−2.3
Max. magnetic field (T)	2.5
Injection scheme	Axial + external ion source
Extraction	protons by stripping extraction
Coils	2 superconductors
Max. current density (A/mm^2)	30
Number of cavities	2
RF harmonic number	4
RF frequency (MHz)	∼61

4 Magnetic Field Model

To begin with, one can take analytical approach and use simple formulae (and assume uniform iron saturation) to calculate major parameters of the magnet, like the number of sectors, B_0 in the machine centre, hill azimuthal width, hill and valley gaps etc, given a maximum energy and extraction radius of the cyclotron. Often a radial sector of zero spiral is assumed at start. And then, spiral angle is added up by using the matrix method to provide enough axial focusing. These calculations give rise to a preliminary geometry of the magnet.

Alternatively, one could bypass the preceding step, instead, just take a shortcut to fudge a magnetic field distribution by simply scaling up or down a well-established cyclotron field map with two scaling factors: one is for the radial size of the magnet, sort of like a conversion factor for the length unit; the other is for the field strength, similar to the coil excitation which changes the field strength linearly. Despite arbitrary values, these two scaling factors

allows to cook up a cartoon machine of suitable magnet size and desired field strength according to the maximum beam energy specified. And then, one can run CYCLOPS on the field map to calculate the equilibrium orbits, for which one needs to adjust the value of B_0 (in the machine centre) to get the resulting isochronism parameter $(\omega_0/\omega - 1)$ to vary around zero [37] over the entire energy range. This would show a poor isochronism of course. And then, one can improve it by modifying the field map in terms of the expression

$$B_{z,\,new}(r,\theta) = \frac{B_{z,\,old}(r,\theta)}{1+\gamma^2\left(\frac{\omega_{old}}{\omega_0}-1\right)}\,, \tag{2}$$

where $B_{z,\,old}(r,\theta)$ and $B_{z,\,new}(r,\theta)$ denote respectively the old and the updated field values along the equilibrium orbit (EO) of relativistic factor γ (corresponding to the energy), ω_{old} denotes the old revolution angular frequency along the EO, while ω_0 denotes the isochronous angular frequency. After iterations, the field isochronism can become significantly improved, converging the parameter $|\omega_0/\omega - 1|$ to the order of 10^{-4} over the full energy range.

Next, one has to employ the electromagnetic field computation software to illustrate the magnet model and the field map, and then further to modify/optimize the geometrical parameters of the structure such as the angular width of the sectors, vertical height and radial extension of the shims, as well as the size of the coils. The iteration repeats until a satisfactory layout is reached in terms of the isochronism, axial focusing, and the fringe field fall-off etc.

Fig. 1 shows the *OPERA* model of the main magnet (1/8), of mirror symmetry with respect to the median plane and 4-fold azimuthal rotational symmetry.

In the geometrical median plane (GMP) the maximum magnetic flux density is ∼2.5 T in the hill. Look at Fig. 2 for the contour of the magnetic flux density and Fig. 3 for the mean field strength versus the radius.

5 Isochronism and Tunes

The isochronism $(\omega_0/\omega - 1)$ of the magnetic field model is better than $\pm 5 \times 10^{-4}$ over the entire acceleration region (except for the centre region and the extraction region). The phase excursion is less than $\pm 44^\circ$ throughout. These are shown in Fig. 4 and Fig. 5.

The magnet shape was optimized to provide a vertical tune rapidly reaching above 0.2 as well as to avoid crossing the coupling resonance $\nu_r - \nu_z = 1$. See Fig. 6 and Fig. 7.

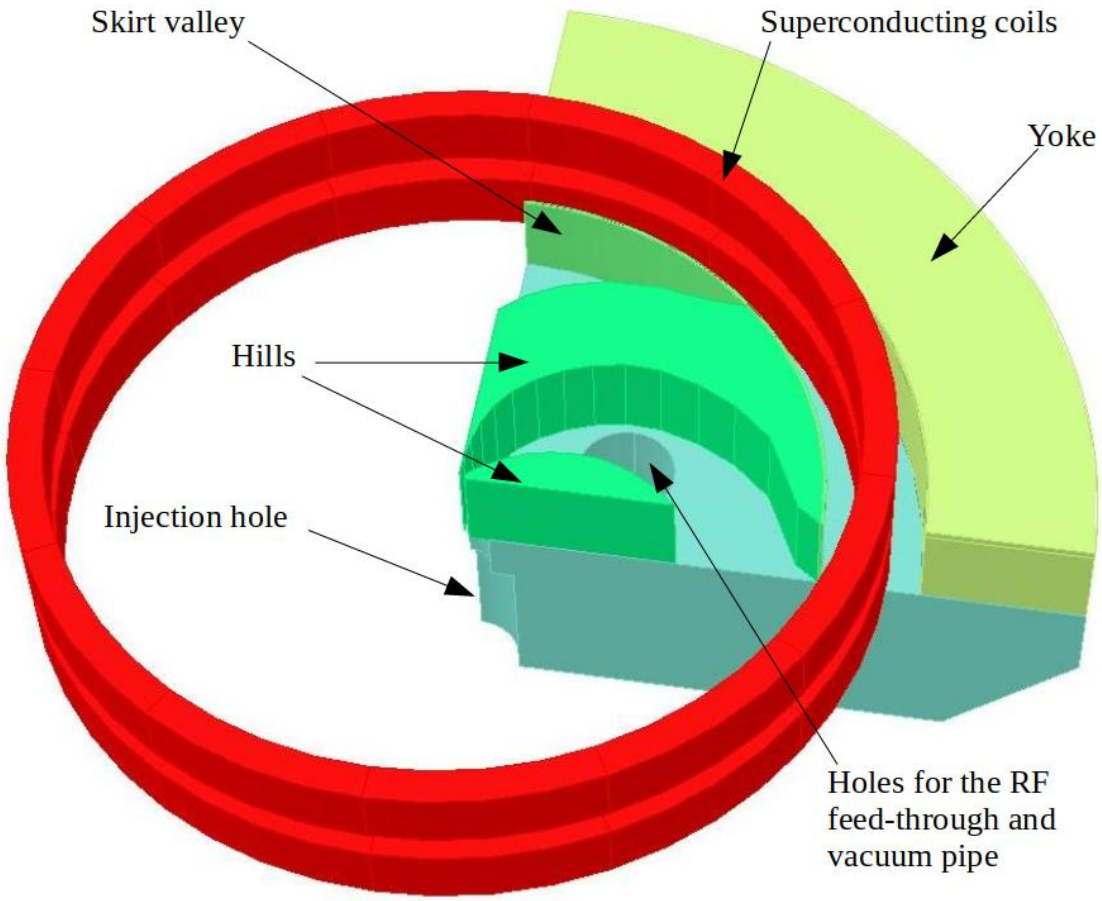

Figure 1: *1/8 OPERA model of the main magnet, mainly composed of the pole with spiral sector, yoke and superconducting coil. For illustrative purpose, here the pole and sector and yoke are represented in different colours but they possess the same material. So is the skirt valley, which is a thin wall structure placed at the outer edge of the spiral sectors, serving to compensate for the isochronous field in the extraction region as well as to create a positive field gradient in the valley region for the beam extraction.*

6 Stripping Extraction

We extract protons by stripping of H_2^+. Placing the stripper properly (on the hill) cannot only pull the protons to the outside of cyclotron in a decent path, but also deliver different energy protons to the same location. Fig. 8 shows extraction trajectories of ∼150 and ∼140 MeV protons. They can arrive at the same cross-over point where the magnetic field falls off to near zero.

The transfer matrices (6×6) along the reference extraction trajectory were calculated, followed by the beam envelope evaluation assuming an emittance of $1.0\,\pi$ mm.mrad (4rms, normalized) for the circulating beam. The proton beam sizes appear smaller than 5 mm in both horizontal and vertical dimensions, well within the pole gap. See Fig. 9. However, after

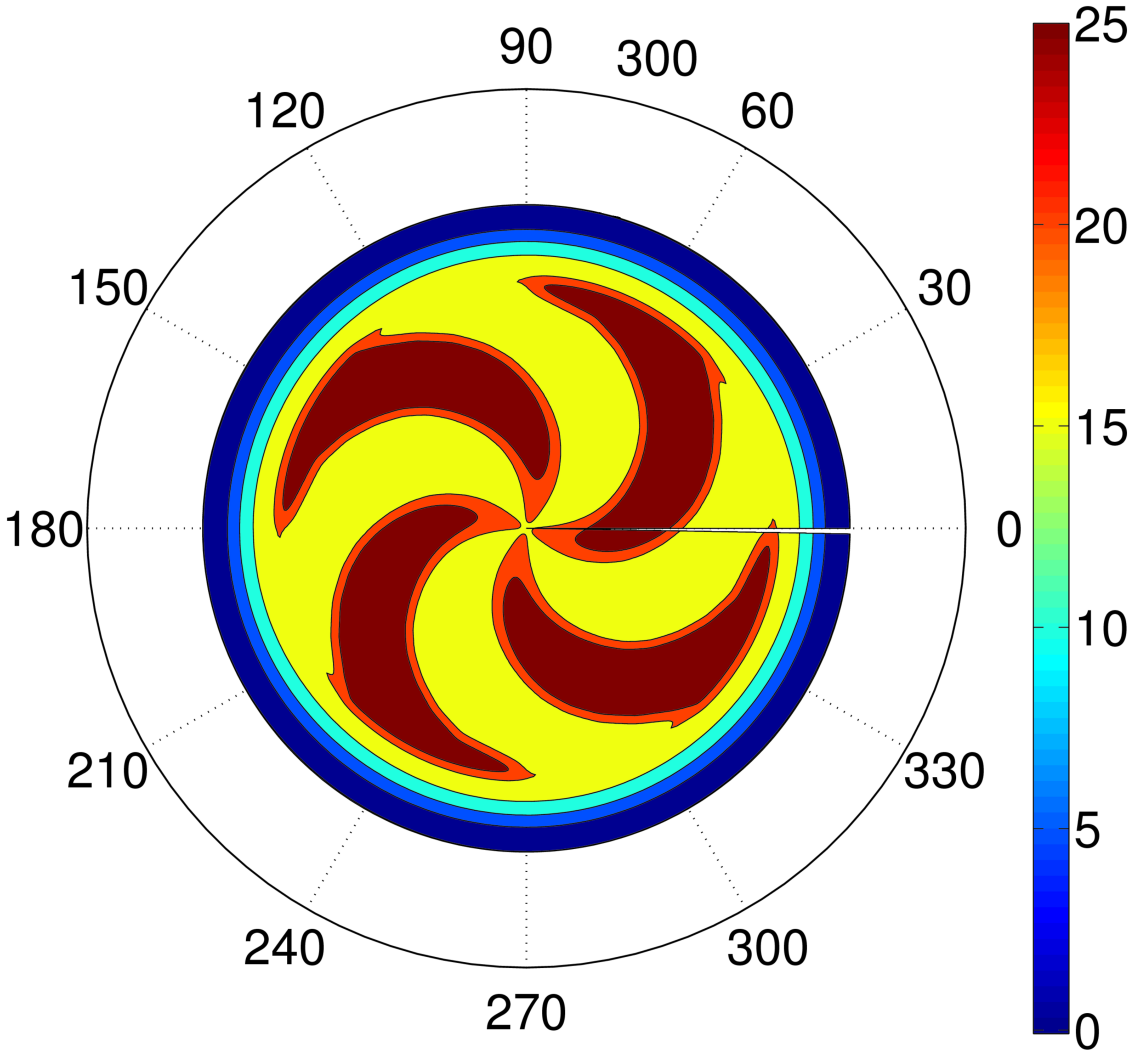

Figure 2: *The contour of $B_z(r, \theta)$ in the median plane. The maximum field strength is ∼2.5 T in the hill.*

entering the fringe field, the radial size gets defocused continuously while the axial size gets over-focused [38]. This means that magnetic channels need to be configured in this area for a compensation.

7 Centre Region

As fore-mentioned, for the TR100+ we purport to replicate the centre region orbits of TR30. This is fulfilled as expected. Fig. 10 shows the resultant first 3-turn's orbits in the median plane for the particles of starting time at 23°, 33°, 43°, 53° and 63°. This result appears to be closely reproduced from that of TR30 [32]. The maximum centring error for the phases in the 40° phase band is 2 mm at turn 10. This is acceptable because it's much smaller

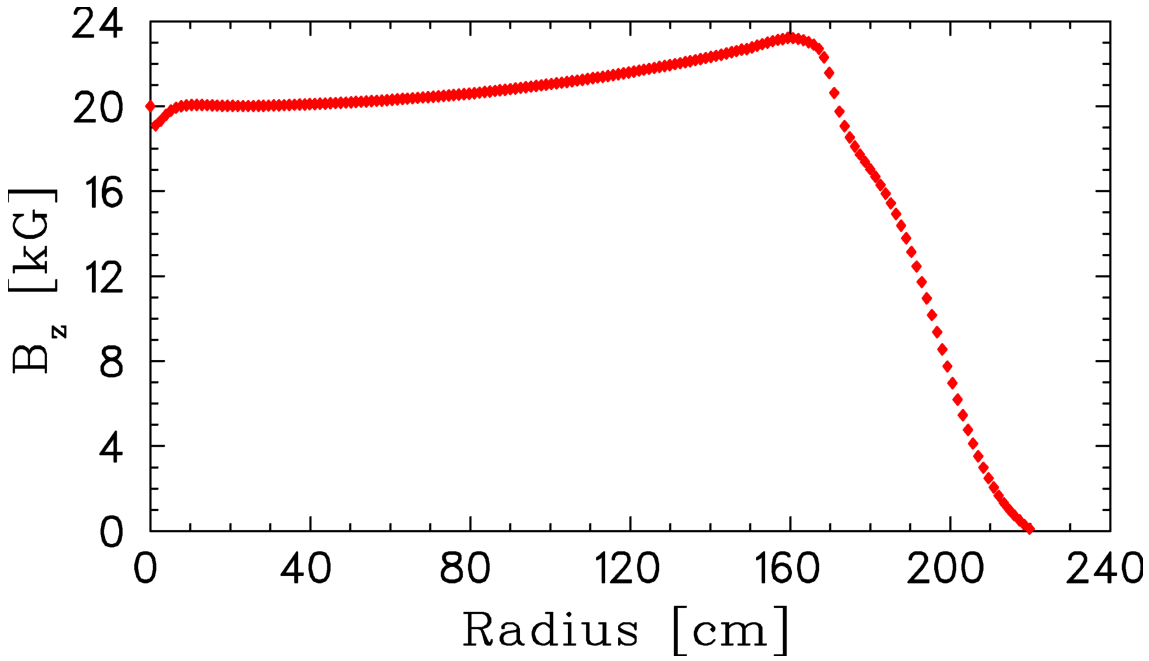

Figure 3: *The average magnetic field strength versus the radius.*

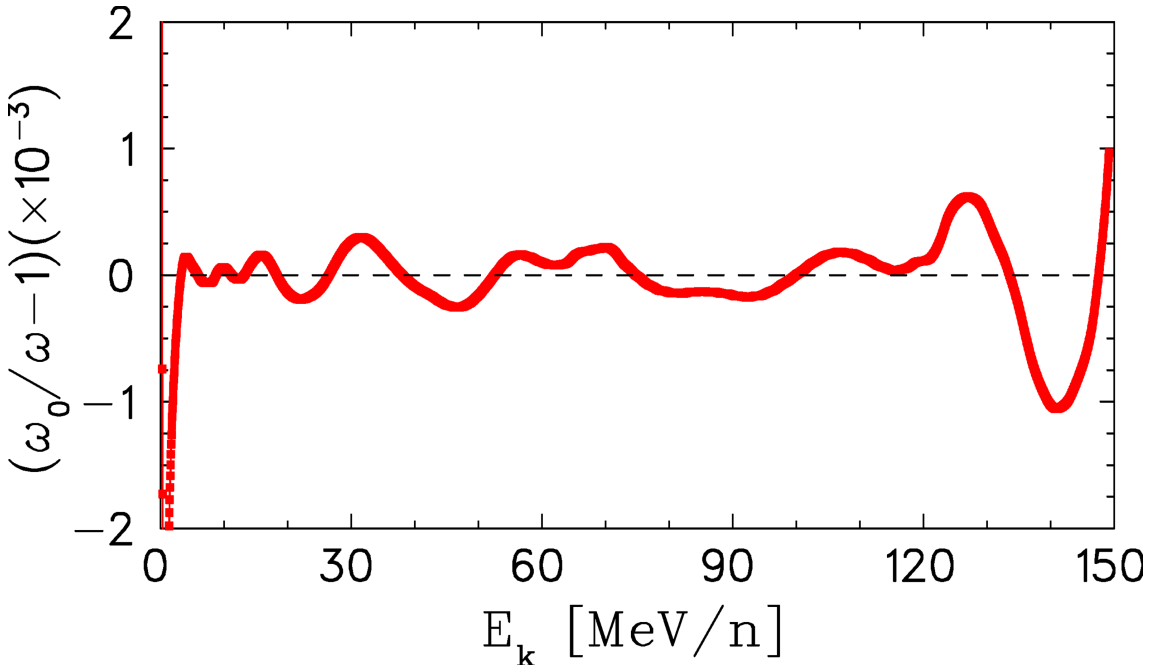

Figure 4: *The isochronism parameter* $(\omega_0/\omega - 1)$ *vs. kinetic energy, where* ω_0 *and* ω *are respectively the isochronous angular frequency and the revolution angular frequency of particle along the SEO.*

than the typical maximum betatron amplitude of ∼10 mm and the centring errors are well grouped together in (x, p_x) space.

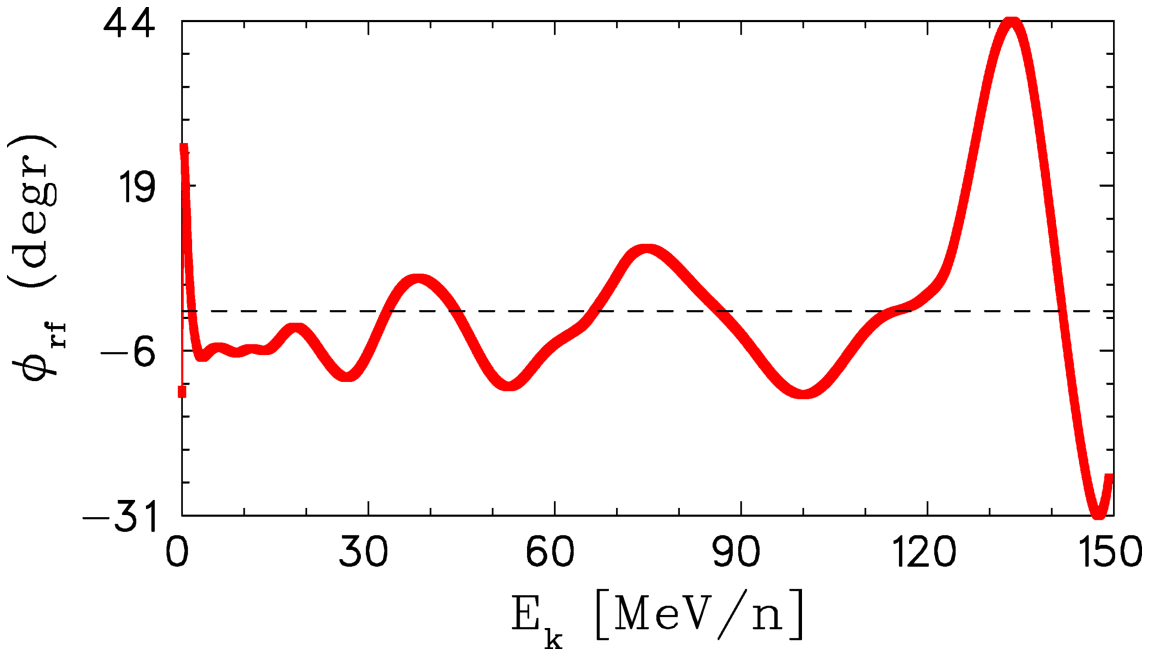

Figure 5: *The rf phase vs. energy, showing that the excursion stays within* $\pm 44°$ *over the entire energy range, assuming a peak energy gain of 0.4 MeV per turn.*

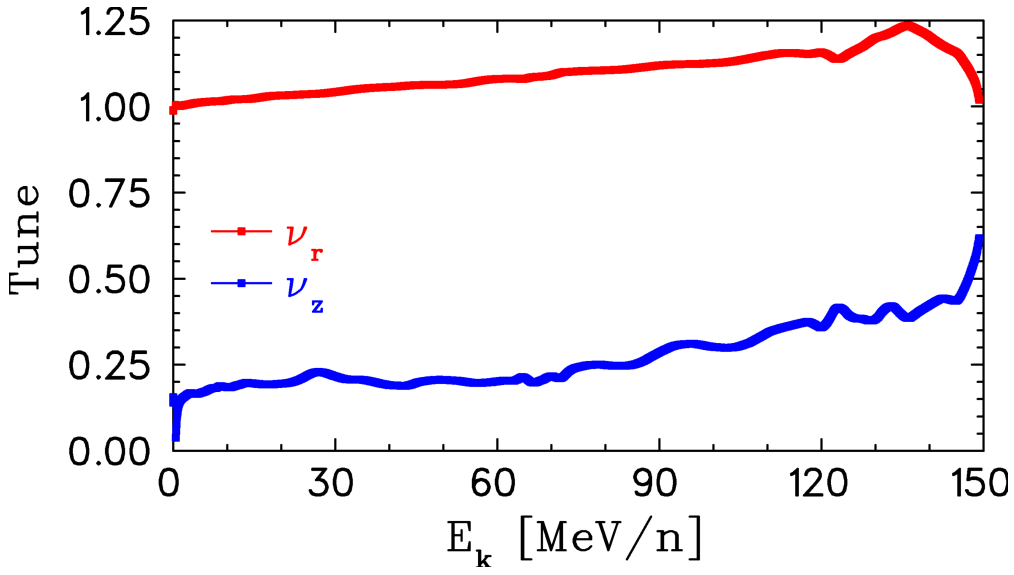

Figure 6: *The* ν_r *and* ν_z *vs. energy.*

In Fig. 11 the vertical motion is shown for the 5 different starting phases of 40° width. We have chosen to show the particles starting with $z = 0$ and $p_z \simeq 0$ respectively with a normalized emittance of $\sim$1.0 πmm-mrad.

Actually we have refined the vertical openings of the first two rf gaps to improve the vertical focusing. Since the ions are accelerated as they cross the gap, they spend more time in the focusing fields near the gap entrance than they do in the defocusing fields near the

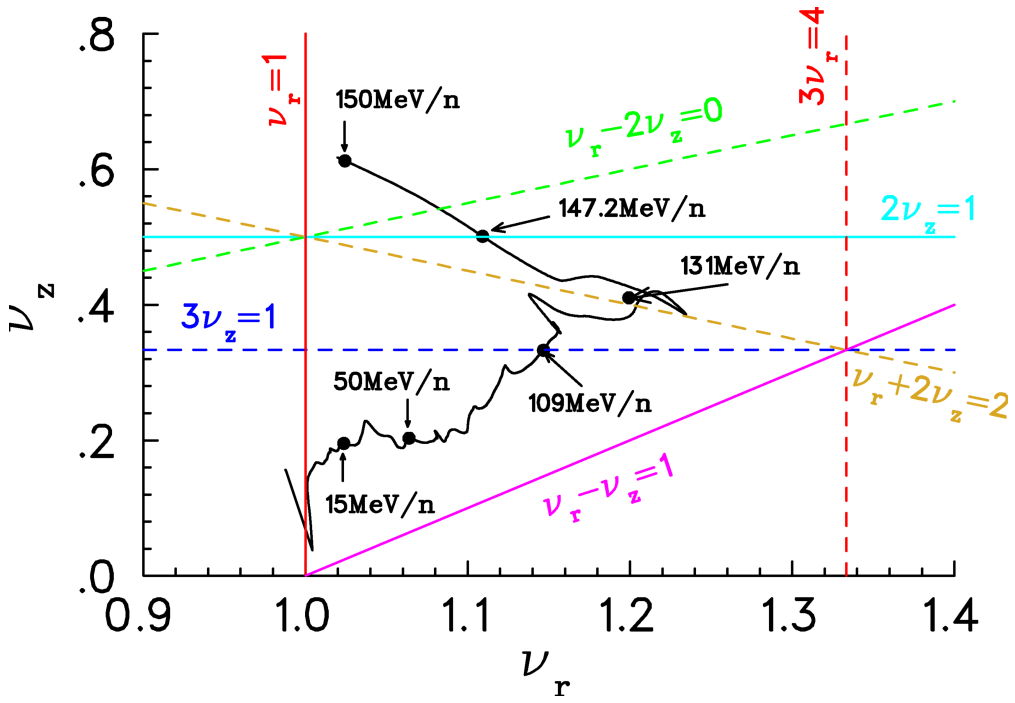

Figure 7: *The tune diagram. Note that the coupling resonance* $\nu_r - \nu_z = 1$ *is avoided; the half-integer resonance* $2\nu_z = 1$ *occurs at* $\sim$*147.2 MeV/n, however.*

gap exit, this produces a net focusing effect. Static focusing arises when the curvature of the equipotentials is greater on one side of the gap than on the other, depending on the apertures. When the vertical equipotentials are more curved at the gap entrance than at the gap exit, the vertical field is greater at the gap entrance than at the gap exit, thus the vertical focusing is augmented. Specifically, we have increased the vertical openings to ± 7.5 mm and ± 10 mm respectively from the original value of ± 5 mm for the first two gap's exits. As a result of these increases, the overall vertical focal power becomes stronger particularly for the particles of leading phases at start. This helps to increase the phase acceptance. See Fig. 12.

8 Spiral Inflector

We modelled an inflector using `CASINO`, assuming a flat B-field throughout. Fig. 13 shows the reference trajectory, and Table 8 lists the inflector's transfer matrix in coordinates (u, p_u, h, p_h, v, p_v).

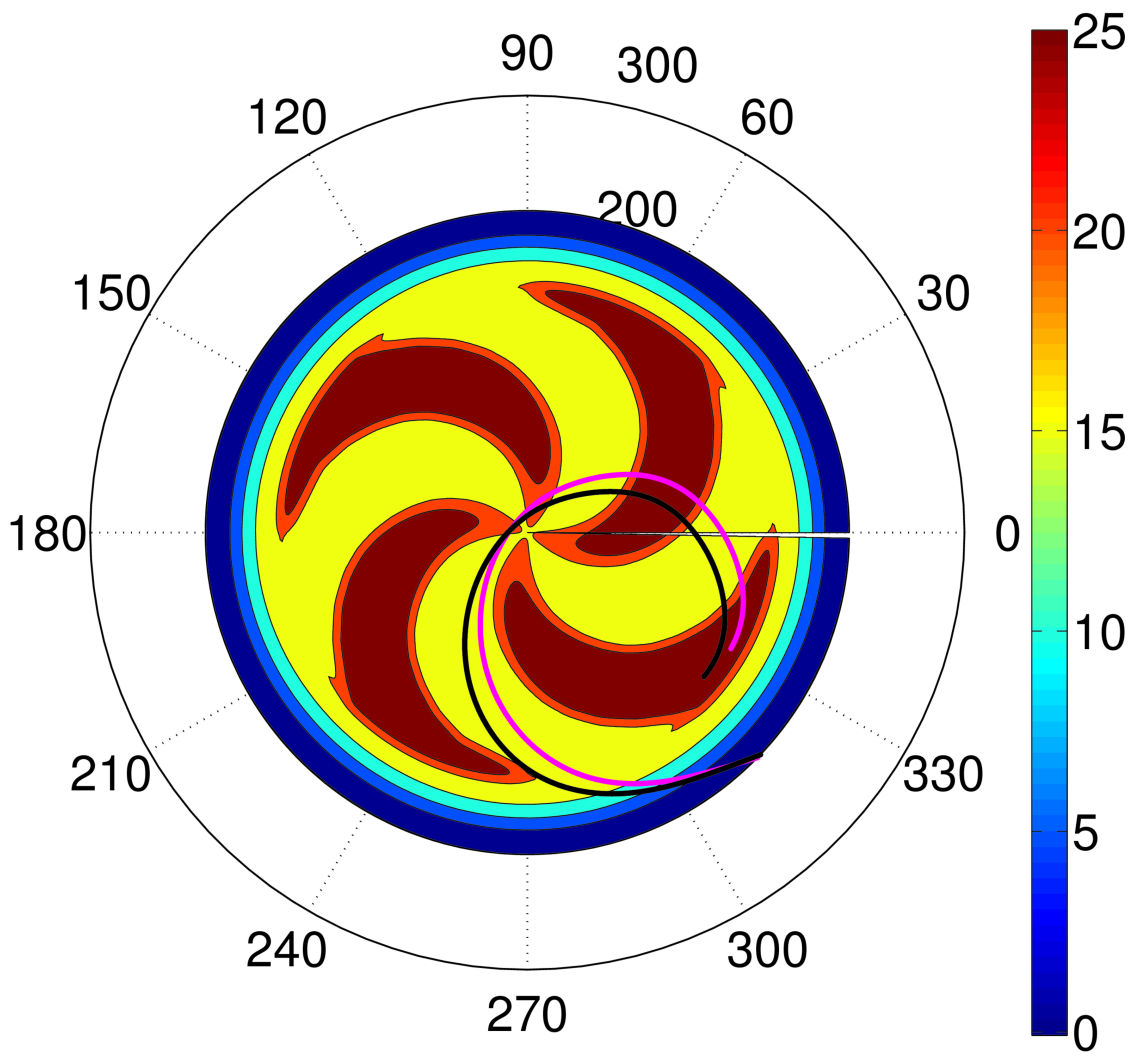

Figure 8: *The extraction trajectories of 150 MeV (magenta) and 140 MeV (black) protons after the circulating H_2^+ is stripped. Both trajectories can arrive at the same location where the field falls off to nearly zero.*

Table 4: Inflector's transfer matrix in the coordinates (u, p_u, h, p_h, v, p_v)

-0.2415333	2.8372763	1.2572299	1.3220140	0.0000000	-7.0175773
-0.1884899	1.6145249	0.5081461	1.2132847	0.0000000	-2.9165501
-0.5627307	0.6675430	0.2976628	-0.8256537	0.0000000	-1.2821949
-0.0170298	-1.4999123	0.2130141	-0.1029479	0.0000000	0.6347262
0.9971232	-1.5555742	-0.3606329	-4.0019058	1.0000000	2.8589376
0.0000000	0.0000000	0.0000000	0.0000000	0.0000000	1.0000000

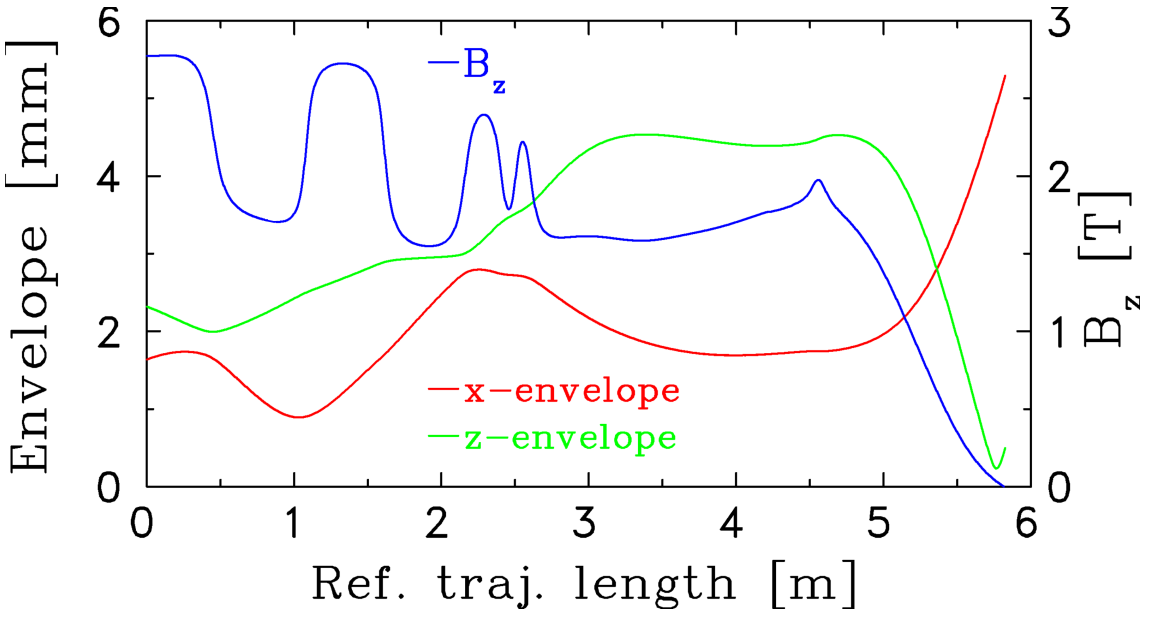

Figure 9: *The horizontal and axial beam envelopes (2rms) of 150 MeV protons. Also shown is the magnetic field strength along the extraction trajectory.*

9 Intensity Limitation

The acceleration process of H_2^+ in a compact cyclotron is similar to that of H^-: in both cases the space charge effects are strongest in the first few turns. The intensity limit is due both to the vertical space charge tune shift and to the longitudinal space charge effect. Both effects give similar upper limits in the TR30 case [39]. The measurements for the TR30 demonstrated 1.0 mA beam current accepted under 5.0 mA injected dc beam. Since TR100+ replicates TR30 centre region geometry and size, it makes sense to use the formula (7) given in [39] for an estimate of the current limit:

$$\hat{I}_{max(vert)} = \beta \left(\frac{\nu_{z0} b_{max}}{R_\infty} \right)^2 \frac{A}{q^2} \left(7.8 \times 10^6 \,\mathrm{Amp} \right) . \tag{3}$$

As listed in Table 3, the ratio of TR100+ to TR30 is 1.2 in R_∞, 0.833 in the injection β, and twice in $\frac{A}{q^2}$. These give 1.16 times the space charge limit of TR30, provided we have the same value of ν_{z0} ($\simeq$0.3) and the same value of aperture half height b_{max} (5 mm). This implies 500 µA H_2^+ expected to be acceptable by the cyclotron under 2.2 mA injected dc beam, and therefore 1.0 mA protons expected from extraction.

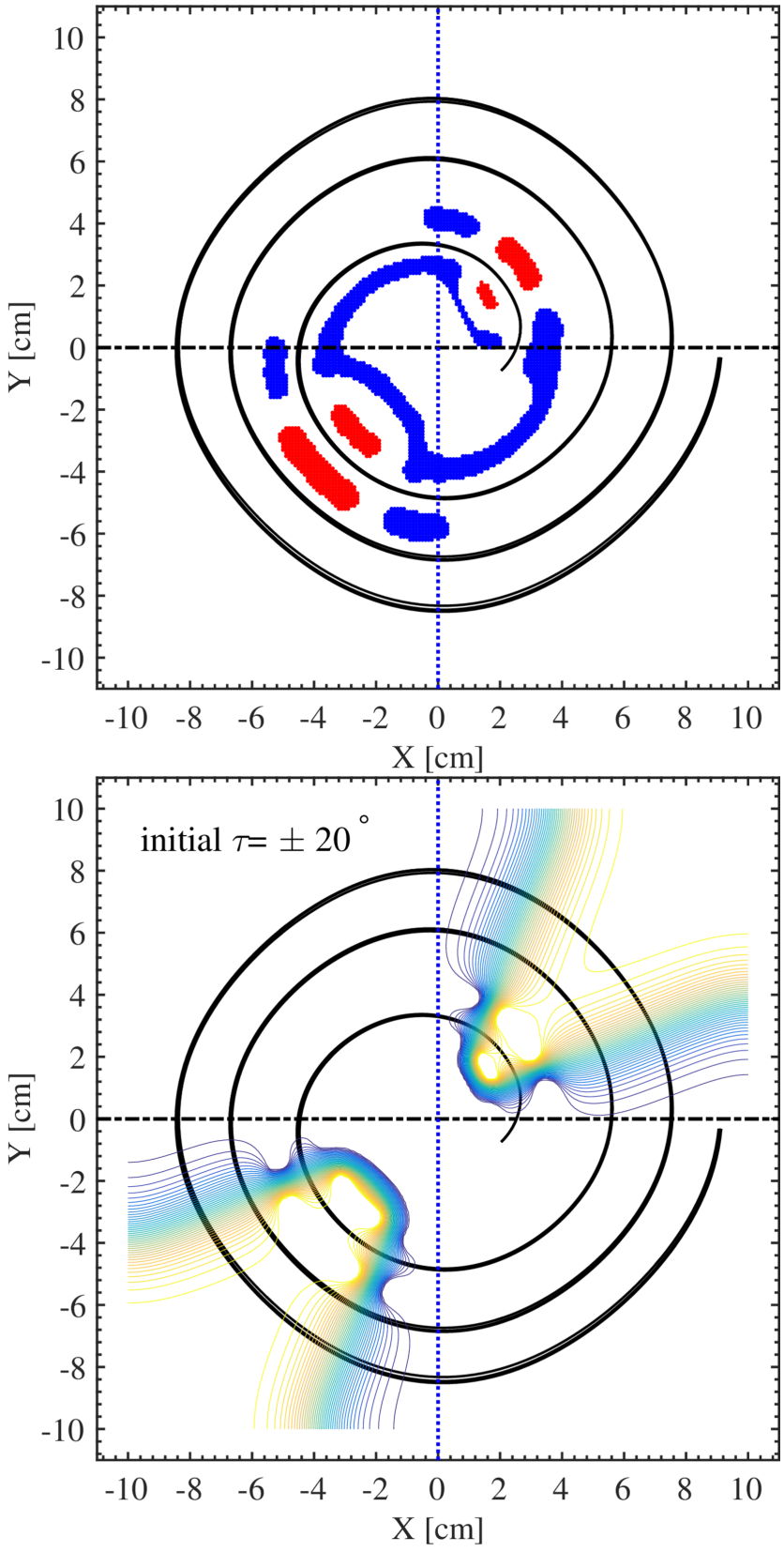

Figure 10: *The first 3-turn's orbits in the median plane for the particles of* 40° *rf phase band at start. Also shown are the central region electrodes in the median plane and the equipotential lines of the electric field.*

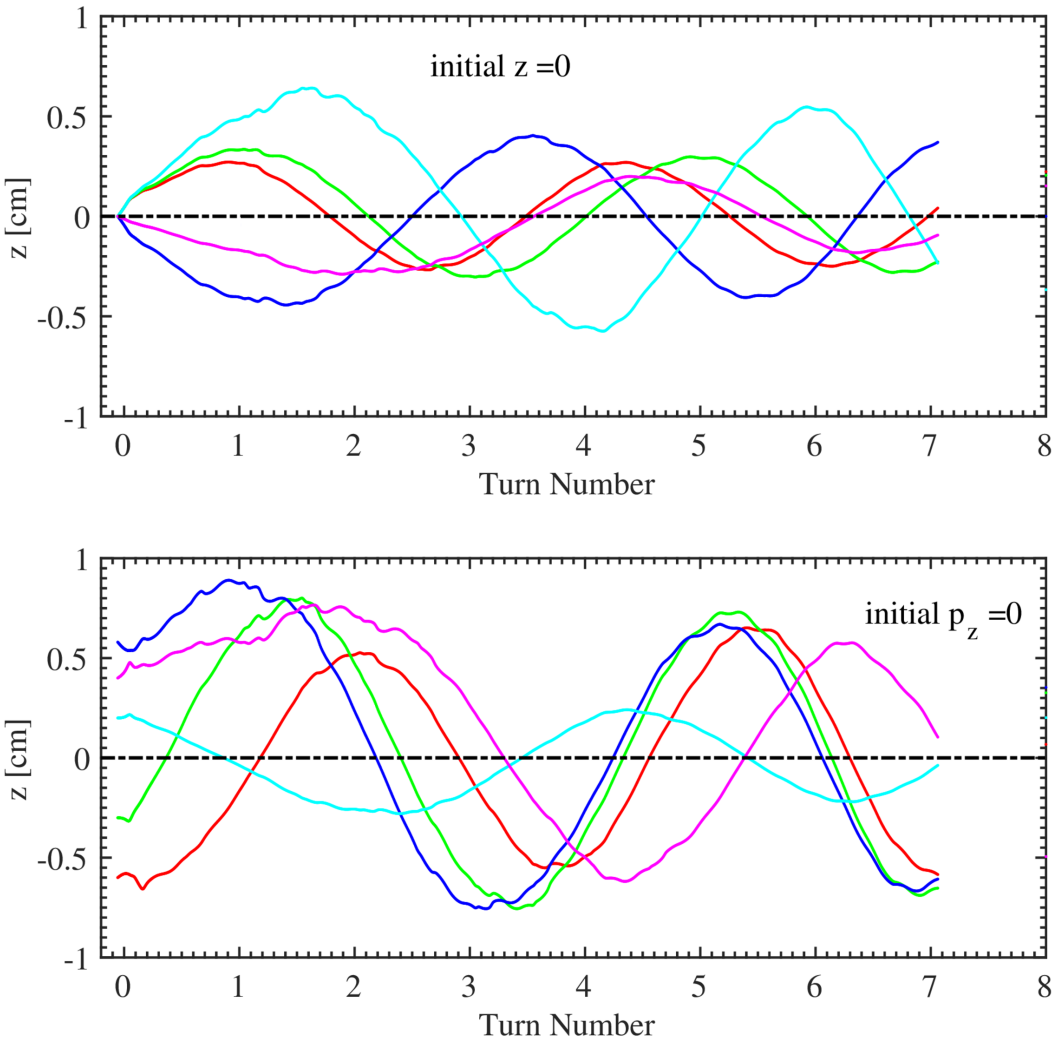

Figure 11: *The first few-turn's vertical motion for the 5 different starting phases.*

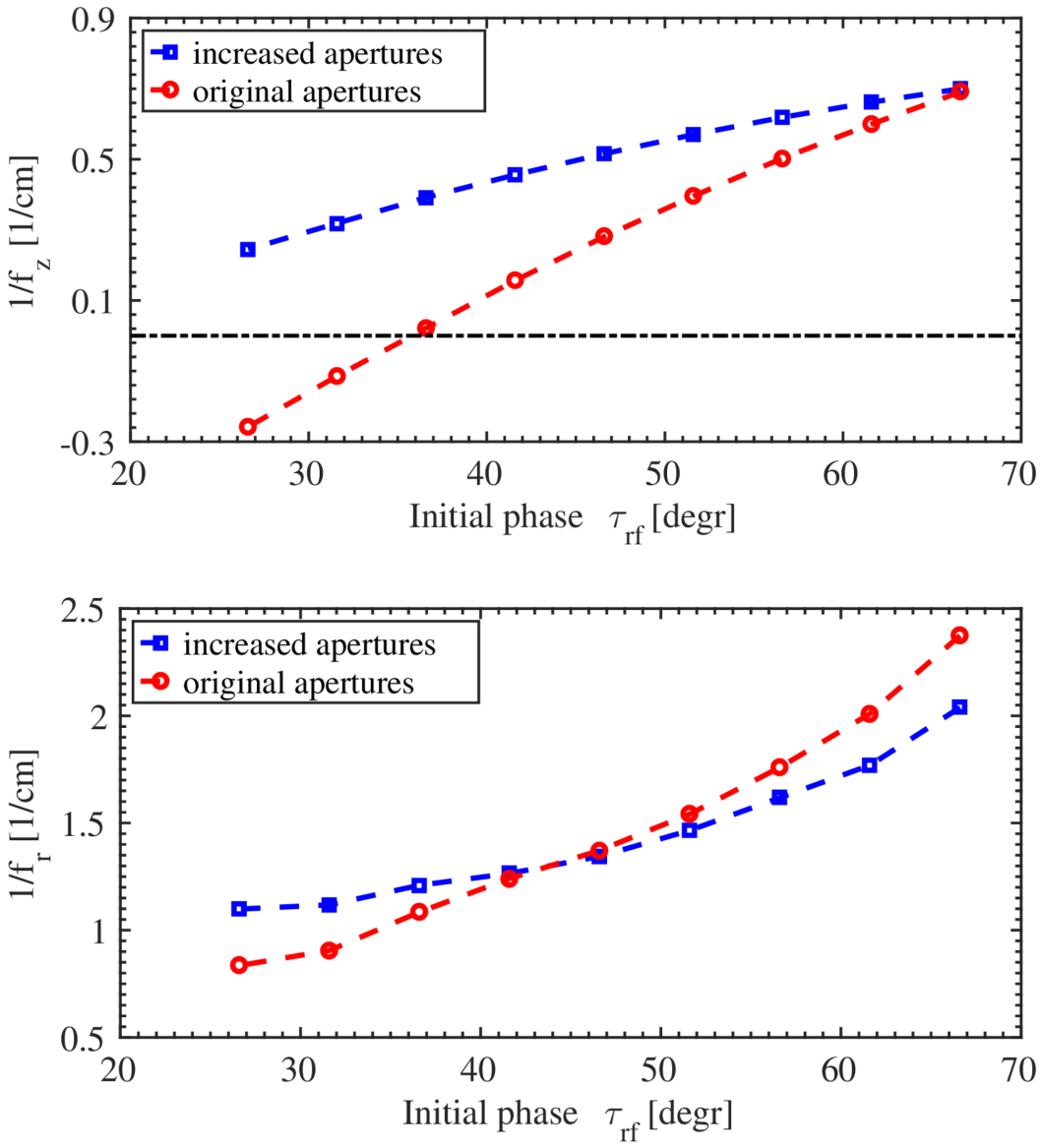

Figure 12: *Overall vertical (upper) and radial (lower) focal power of the first two gaps versus the starting phase of the particle, before and after increasing the apertures. It's seen that the vertical focusing is augmented especially for the particles of leading phases.*

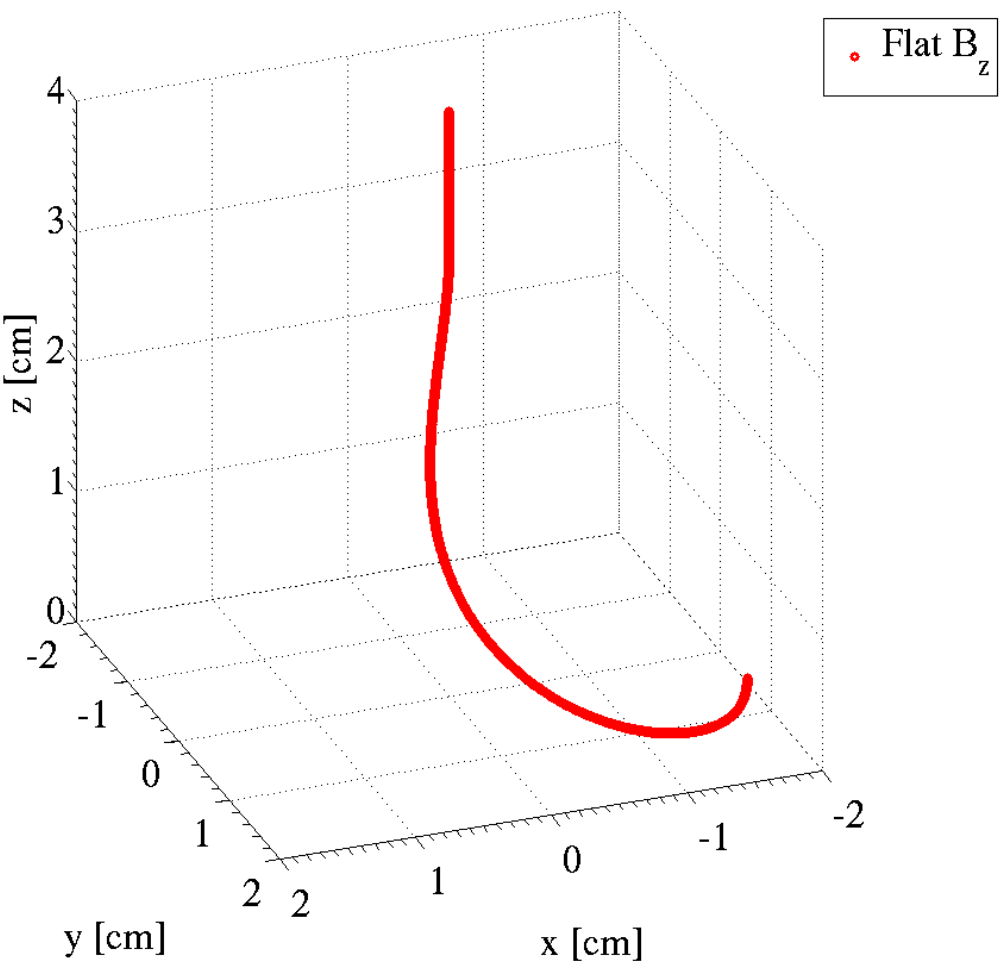

Figure 13: *The reference trajectory through the inflector.*

10 Beam Losses

Two types of H_2^+ beam loss are concerned: the electromagnetic dissociation (Lorentz stripping) and the interactions with residual gas. The binding energy of the last electron is 2.75 eV, ∼3.6 times larger than the binding energy in the H^- case. This bind can be dissociated by the electric field, generated from the motion of the ion in the magnetic field. The effective electric field in the rest frame of the ion is represented as

$$E = 3\beta\gamma B \ , \tag{4}$$

where β and γ are relativistic factors of the ion motion in a magnetic field B in Tesla, and the electric field is given in MV/cm. For 150 MeV/n H_2^+ ions travelling in a 2.5 Tesla magnetic field, the electric field is 1.5 MV/cm. This could dissociate the ions in the vibrational states of $\nu \geq 16$ in terms of Hiskes' model [21], causing ∼0.5% beam loss. See Fig. 14 and Fig. 15.

However, the literature shows that in the ion sources only the low states are populated. See the reference [40] for example. It shows that by mixing some helium into the ion source gas,

the collison-induced dissociation reaction of H_2^+ ions on the He atoms, $H_2^+(\nu)$ + He $\rightarrow$ H^+ + H + He, is exothermic for the higher vibrational states but is endothermic by 2.65 eV for the low states, leaving ν =0, 1 and 2 for 20% mixture. This is an encouraging result for the post-acceleration of H_2^+ ions in an e.g. superconducting cyclotron; with this scheme one loses 50% of the H_2^+ ions, though.

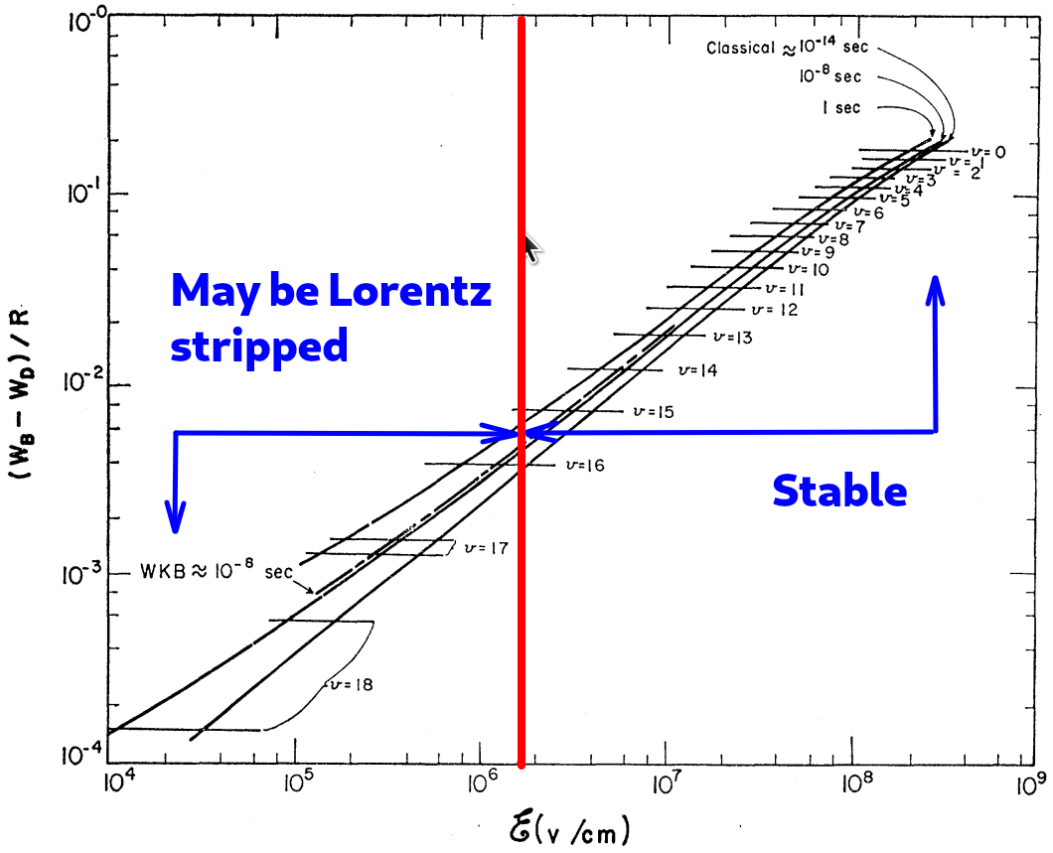

Figure 14: *The Hiskes' plot. The x-axis is the electric field. The y-axis is the binding energy in peculiar unit. The vibrational states that appear entirely to the right of the vertical line in red will survive our maximum electric field from the 150 MeV/n H_2^+ ions in the 2.5 T field.*

The circulating H_2^+ ions can lose their orbital electron as they travel along the acceleration path due to interactions with the residual gas. The fractional beam particles which survive is given by [41]

$$\frac{N}{N_0} = \exp\left(-3.35 \times 10^{16} \int \sigma_L(E)\, P\, dL\right) , \tag{5}$$

where P is the vacuum pressure in torr (3.35×10^{16} is the number of molecules/cm^3/torr), and L is the path length in cm. The cross section of electron loss is

$$\sigma_L(E) = 4\pi a_0^2 \left(\frac{V_0}{V}\right)^2 \frac{Z_t^2 + Z_t}{Z_i} , \tag{6}$$

where V is the ion velocity, while V_0 and a_0 are the characteristic Bohr velocity and radius. Z_t and Z_i are the atomic number of the residual gas and of the incident ion respectively.

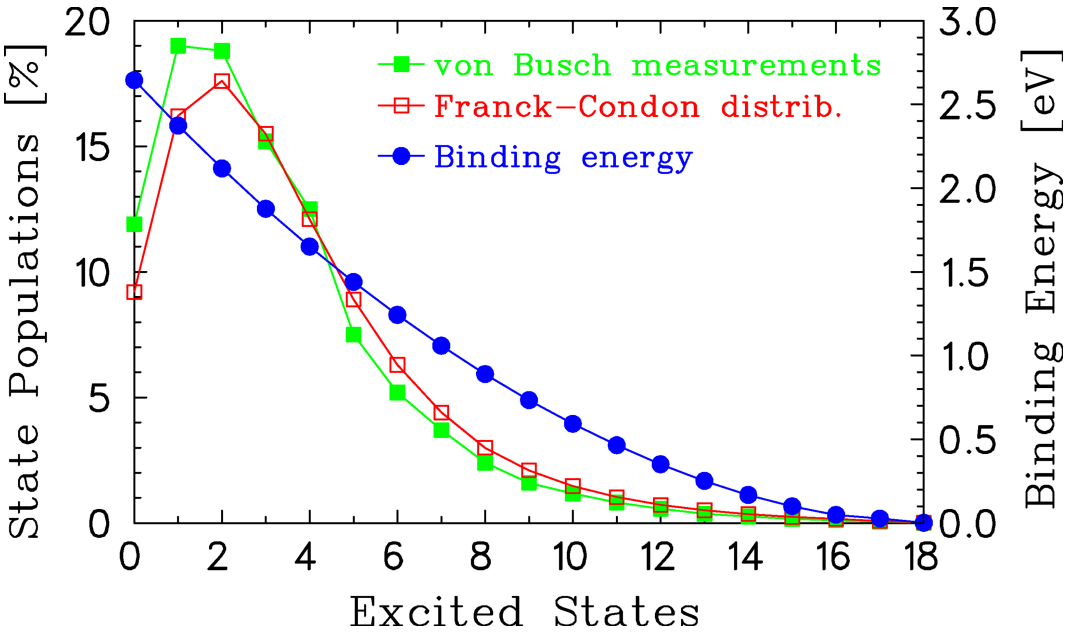

Figure 15: *The H_2^+ ion vibrational state's populations and binding energy, plotted from Busch and Dunn [42].*

With these equations, we estimate that the vacuum has to be better than 5.0×10^{-8} torr in order to keep the loss below 0.5% during acceleration.

11 Summary and Outlook

A preliminary design has been carried out to evaluate the feasibility of building a superconducting cyclotron to accelerate H_2^+ beam up to 150 MeV/n, by stripping extraction to deliver protons of 1 mA. The design goal seems workable with the present technology. The proton beam envelope during the extraction of looks pretty decent; further study is needed to improve the focusing in the machine fringe field, though. Besides, further optimization of the sector spiral shape and of the coils will pursue to refine the vertical focusing, taking into account the design of rf cavities to be operated at high voltage and high power. Regarding the electromagnetic stripping of H_2^+, the electric field we are discussing is in the 1-2 MV/cm range. This requires vibrational states of $\nu < 15$ in terms of Hiskes' theory. At least 99.5% H_2^+ beam can survive from the Lorentz stripping. One should probably consider mixing in helium in the ion source to remove the high vibrational states before start of the acceleration process.

12 Acknowledgements

We appreicate Y. Bylinsky, R. Baartman and T. Planche for the discussions.

References

[1] L. CALABRETTA, D. RIFUGGIATO, *SUPERCONDUCTING CYCLOTRONS FOR ACCELERATION OF H_2^+* , Proc. of the 15th Int. Conf. on Cyclotrons and their Applications 1998, 665-668 (1998).

[2] L. Calabretta et al., *HIGH INTENSITY PROTON BEAMS FROM CYCLOTRONS FOR H_2^+* , Proc. of the PAC 1999, 3288-3290 (1999).

[3] L. Calabretta et al., *A SUPERCONDUCTING RING CYCLOTRON TO DELIVER HIGH INTENSITY PROTON BEAMS* , Proc. of the EPAC 2000, 918-920 (2000).

[4] F. Meot et al., *MW-class 800 MeV/n molecular H_2^+ cyclotron for ADS-Reactor application: Challenges and design studies* , Proc. of the IPAC 2012, 4121-4123 (2012).

[5] J.W. Weidner et al., *^{225}Ac and ^{223}Ra production via 800 MeV proton irradiation of natural thorium targets*, Applied Radiation and Isotopes, 70 (2012) 2590–2595.

[6] TRIUMF, BC Cancer Agency, et al., *Canadian Team Demonstrates Solution to Medical Isotope Crisis,* News Release, For Immediate Release, January 5, 2015. https://www.triumf.ca/sites/default/files/2015-01-05_NR-ITAP-Milestone_vFINAL_0.pdf.

[7] P. Schaffer et al., *Direct Production of ^{99m}Tc via ^{100}Mo(p,2n) on Small Medical Cyclotrons,* Physics Procedia 66 (2015) 383–395.

[8] Francois Bénard et al., *Implementation of Multi-Curie Production of ^{99m}Tc by Conventional Medical Cyclotrons,* The Journal of Nuclear Medicine, Vol.55 No.6, 1017–1022, 2014.

[9] Thomas J. Ruth, *The Medical Isotope Crisis: How We Got Here and Where We Are Going,* Journal of Nuclear Medicine Technology Vol.42 No.4, 245–248, 2014.

[10] P.W. Schmor, *REVIEW OF CYCLOTRONS USED IN THE PRODUCTION OF RADIOISOTOPES FOR BIOMEDICAL APPLICATIONS*, Proc. of CYCLOTRONS 2010, 413 (2010).

[11] V. Sabaiduc et al., *NEW HIGH INTENSITY COMPACT NEGATIVE HYDROGEN ION CYCLOTRONS* , Proc. of CYCLOTRONS 2010, 81 (2010).

[12] J. Martino, *ARRONAX*, A HIGH INTENSITY CYCLOTRON IN NANTES*, Proc. of 18th Int. Conf. on Cyclotrons and their Applications 2007, 215 (2007).

[13] Tianjue Zhang *et al.*, *Design & construction status of CYCIAE-100, a 100 MeV H^- cyclotron for RIB production*, Nucl. Instrum. Methods Phys. Res., Sect. B, vol. 266, pp. 4117–4122 (2008).

[14] G.M. Stinson et al., *Electric dissociation of H^- ions by magnetic fields*, Nucl. Instr. and Meth. 74 (1969) 333-341.

[15] Bruce F. Milton, *COMMERCIAL COMPACT CYCLOTRONS IN THE '90s* , Proc. of the 14th Int. Conf. on Cyclotrons and their Applications 1995, 99 (1995).

[16] H.-U. Klein et al., *Design, Manufacturing and Commissioning of Compact Superconducting 250 MeV Cyclotrons for Proton Therapy: A Short Report from the Field* , IEEE/CSC & ESAS EUROPEAN SUPERCONDUCTIVITY NEWS FORUM, 2 (2007).

[17] W. Beeckman et al., *Preliminary design of a reduced cost proton therapy facility using a compact, high field isochronous cyclotron* , Nuclear Instruments and Methods in Physics Research B56/57 (1991) 1201-1204.

[18] Yves Jongen *REVIEW ON CYCLOTRONS FOR CANCER THERAPY* , Proc. of CYCLOTRONS 2010, 398-403 (2010).

[19] M. Seidel and P.A. Schmelzbach, *Upgrade of the PSI Cyclotron Facility to 1.8 MW,* , Proc. 18th Int. Conf. on Cyclotrons and Their Applications 2007, 157 (2007).

[20] Y. Jongen, *THE PROTON THERAPY SYSTEM FOR MGH'S NPTC: EQUIPMENT DESCRIPTION AND PROGRESS REPORT*, Proc. of the 14th Int. Conf. on Cyclotrons and their Applications 1995, 606-609 (1995).

[21] J. R. Hiskes, *Dissociation of Molecular Ions by Electric and Magnetic Fields*, Phys. Rev., vol. 122, pp. 1207-1217, May 1961.

[22] H. H. Harris et al., *Binding Energy of* H_3^+, J. Chem. Phys. 59 (1973) 6181.

[23] Jose R. Alonso, *High Current* H_2^+ *Cyclotrons for Neutrino Physics: The IsoDAR and DAEδALUS Projects** , Proc. of 22nd Int. Conf. on the Application of Accelerators in Research and Industry (CAARI), Ft. Worth, TX, Aug 5-10, 2012.

[24] P. Mandrillon, M. Conjat, *SINGLE STAGE CYCLOTRON FOR AN ADS* , Proceedings of Cyclotrons2016, 387-393 (2016).

[25] M. Maggiore et al., *PROGRESS ON THE DESIGN STUDIES OF THE 300 AMeV SUPERCONDUCTING CYCLOTRON* , Proc. of Proc. of the 18th Int. Conf. on Cyclotrons and their Applications 2007, 163-165 (2007).

[26] G.N. Vialov, G.N. Flerov, Y.Tz. Oganessian, JINR Preprint No. 1884, Dubna, 1964.

[27] G.G. Gulbekyan et al., *Extraction By Stripping of Heavy Ion Beams From Avf Cyclotrons,* Proc. of Cyclotrons 2007, 308–313 (2007).

[28] L. Calabretta et al., *A novel superconducting cyclotron for therapy and radioisotope production* , Nucl. Instr. and Meth. in Phys. Research A 562 (2006) 1009–1012.

[29] M. Abs et al., *Multi-Megawatt DAEδALUS Cyclotrons for Neutrino Physics*, arXiv:1207.4895 (2012).

[30] D. Winklehner, *UPDATED PHYSICS DESIGN OF THE DAEδALUS AND IsoDAR COUPLED CYCLOTRONS FOR HIGH INTENSITY* H_2^+ *BEAM PRODUCTION*, arXiv:1708.06412 (2017).

[31] H. Hus et al., *Dissociative Recombination of Electrons with H_2^+ in Low Vibrational States,* Phys. Rev. Lett., Vol. 60, 1006–1009 (1988).

[32] R. Baartman et al., *A 30 MeV H^- CYCLOTRON FOR ISOTOPES PRODUCTION*, Proceedings of the Particle Accelerator Conference 1989, p.1623-1625.

[33] A.E. Geisler et al., *COMMISSIONING OF THE ACCEL 250 MEV PROTON CYCLOTRON*, Proceedings of the Eighteenth Int. Conf. on Cyclotrons and their Applications, 2007, p.9-14.

[34] B.F. Milton et al., *Commissioning and First Operation of a 500 μA, 30 MeV, H^- Cyclotron: The TR30*, Proceedings of the IEEE Particle Accelerator Conference 1991, p.65-67.

[35] Leandro A.C. Piazza, *SCENT 300 Project Status Review*, XXXVII ECPM, 29-10-2009.

[36] Y. Jongen et al., *Compact superconducting cyclotron C400 for hardron therapy* , Nucl. Instr. and Meth. in Phys. Research A 624 (2010) 47-53.

[37] Y.-N. Rao, *On Cyclotron Orbit Calculations*, TRIUMF Beam Physics Note TRI-BN-19-14, Mar. 4, 2019.

[38] Y.-N. Rao et al., *CONCEPTUAL DESIGN OF TR100+: AN INNOVATIVE SUPERCONDUCTING CYCLOTRON FOR COMMERCIAL ISOTOPES PRODUCTION*, Proceedings of 22nd Int. Conf. on Cyclotrons and their Applications, Cape Town, South Africa, 2019, pp. 298–301

[39] R. Baartman, *Intensity Limitations in Compact H^- Cyclotrons*, Proc. Cyclotrons'95, Cape Town, South Africa, Oct. 1995, pp. 440–445.

[40] Amarjit Sen, J W McGowan and J B A Mitchell, *Production of low-vibrational-state H_2^+ ions for collision studies*, J. Phys. B: At. Mol. Phys. 20 (1987) 1509-1515.

[41] H.-D. Betz, *Charge States and Charge-Changing Cross Sections of Fast Heavy Ions Penetrating Through Gaseous and Solid Media*, Rev. Mod. Phys., vol. 44, pp. 465-539, Sep. 1972.

[42] Friedrich von Busch and Gordon H. Dunn, *Photodissociation of H_2^+ and D_2^+: Experiment*, Phys. Rev. A, vol. 5 No.4, pp. 1726-1743, 1972.